Nonhistological Diagnosis of Human Cerebral Tumors by ^{1}H Magnetic Resonance Spectroscopy and Amino Acid Analysis[1]

José M. Roda, José M. Pascual, Fernando Carceller, Francisco González-Llanos, Antonio Pérez-Higueras, Juan Solivera, Laura Barrios, and Sebastián Cerdán[2]

Servicio de Neurocirugía, Hospital Universitario La Paz, E-28046 Madrid [J. M. R., J. M. P., F. C., F. G-L., J. S.]; Fundación Jiménez Díaz, E-28040 Madrid [A. P-H.]; Centro Técnico de Informática Consejo Superior de Investigaciones Científicas (C.S.I.C.), E-28006 Madrid [L. B.]; and Instituto de Investigaciones Biomédicas, C.S.I.C., E-28029 Madrid [S. C.], Spain

ABSTRACT

We describe a multivariate analysis procedure to classify human cerebral tumors nonhistologically *in vitro*, combining the use of ^{1}H magnetic resonance spectroscopy (MRS) with automatic amino acid analysis of biopsy extracts. Eighty-one biopsies were obtained surgically and classified histologically in eight classes: high-grade astrocytomas (class 1, $n = 19$), low-grade astrocytomas (class 2, $n = 10$), normal brain (class 3, $n = 9$), medulloblastomas (class 4, $n = 4$), meningiomas (class 5, $n = 18$), metastases (class 6, $n = 8$), neurinomas (class 7, $n = 9$), and oligodendrogliomas (class 8, $n = 4$). Perchloric acid extracts were prepared from every biopsy and analyzed by high resolution ^{1}H MRS and automatic amino acid analysis by ionic exchange chromatography. Intensities of 27 resonances and ratios of resonances were measured in the ^{1}H MRS spectra, and 17 amino acid concentrations were determined in the chromatograms. Linear discriminant analysis provided the most adequate combination of these variables for binary classifications of a biopsy between any two possible classes and in multiple choice comparisons, involving the eight possible classes considered. Correct diagnosis was obtained when the class selected by the computer matched the histological diagnosis. In binary comparisons, consideration of the amino acid profile increased the percentage of correct classifications, being always higher than 75% and reaching 100% in many cases. In multilateral comparisons, scores were: high-grade astrocytomas, 80%; low-grade astrocytomas, 74%; normal brain, 100%; medulloblastomas, 100%; meningiomas, 94.5%; metastases, 86%; neurinomas, 100%; and oligodendrogliomas, 75%. These results indicate that statistical multivariate procedures, combining ^{1}H MRS and amino acid analysis of tissue extracts, provide a valuable classifier for the nonhistological diagnosis of biopsies from brain tumors *in vitro*.

INTRODUCTION

Although tumor diagnosis is traditionally accomplished using well-established histological procedures, the development of nonhistological methods of diagnosis is receiving increasing attention to provide complementary criteria for histopathological evaluations and to explore new protocols of instrumental diagnosis with minimal operator interventions. Using nonhistological procedures, the investigator assumes that the biochemical composition of the tissue is a direct reflection of its cellularity and pathophysiological status, providing diagnostic assignments based on the use of molecular or metabolic profiles rather than on histological patterns. Areas under development include the use of molecular genetic markers (1), isoenzyme patterns (2) or *in vivo* (3–5) and *in vitro* (6–11) MRS[3] approaches for tumor identification.

In vitro ^{1}H MRS of biopsy extracts has been classically used in the nonhistological characterization of brain tumors. In many cases, the discrimination among different tumor classes was based on the analysis and quantification of one resonance or a few resonances from the spectra (6, 12–16). However, the number of resonances in the ^{1}H spectra of tumors *in vitro* is large, and many of them appear to be modified simultaneously in different tumor pathologies (9, 10). This circumstance led to the problem as to how to select the most appropriate resonance or combination of resonances for the classification process. Several chemometric strategies were proposed including statistical multivariate analysis or artificial intelligence techniques such as neural networks, pattern recognition, and cluster analysis (17–21). Nevertheless, unambiguous ^{1}H MRS classifications of tumor biopsies into specific tumor types and grades remained difficult to obtain, even in the simplest cases involving binary classifications of a biopsy between two rival tumor types or grades.

To improve previous approaches to the classification of biopsy extracts, we complemented the information obtained by ^{1}H MRS with that provided by automatic amino acid analysis and explored a novel algorithm to extend the conventional binary comparisons to multilateral comparisons among all of the tissue types present in the database. Amino acid profiles were

Received 1/7/00; revised 5/26/00; accepted 7/18/00.

The costs of publication of this article were defrayed in part by the payment of page charges. This article must therefore be hereby marked *advertisement* in accordance with 18 U.S.C. Section 1734 solely to indicate this fact.

[1] Supported in part by grants from the Community of Madrid 08.1/0023/97 and 08.1/0046/98.

[2] To whom requests for reprints should be addressed, at Instituto de Investigaciones Biomédicas, c/Arturo Duperier 4, E-28029 Madrid, Spain. Phone: 34-91-585-4633; Fax: 34-91-585-4587; Email: scerdan@iib.uam.es.

[3] The abbreviations used are: MRS, magnetic resonance spectroscopy; LOO, Leave One Out (method).

chosen because of the large amount of information available from amino acid metabolism in tumors (22–24), the routine availability of amino acid analyzers in many clinical settings, and the possibility of correlating these results directly with those of ^{1}H MRS, because many amino acids are detectable by both techniques. Consideration of the amino acid profile improved the scores for binary classifications obtained when using ^{1}H MRS data only, and a novel algorithm allowed us to perform multilateral classifications of tissue biopsies with certainties similar to, or in some cases even superior to, those obtained in binary comparisons. These results provide a promising background for the nonhistological diagnosis of human cerebral tumors *in vitro*.

MATERIALS AND METHODS

Preparation and Characterization of Biopsies. Samples from normal human brain and different tumoral tissues were obtained after craniotomy. Once the tissue was selected, a biopsy was taken from the brain or solid portion of the tumor, without previous coagulation to avoid possible interferences of heat and ischemia. Samples were immediately frozen in liquid nitrogen and were stored at −70°C until further processing. Normal brain biopsies were obtained from patients operated on for epilepsy or with neoplasms requiring lobectomy for their removal. In these cases, samples were taken from regions sufficiently far away from the lesion. In tumor samples, a portion of the tumor adjacent to the biopsy, taken for MRS and amino acid analysis, was used for histological diagnosis by the neuropathology section of the hospital. Astrocytoma grading followed the St Anne-Mayo criteria (25), grades 1 and 2 being grouped as "low-grade astrocytomas" and grades 3 and 4 as "high-grade astrocytomas," independently of hemispheric or cerebellar location and patient age. The remaining tumors were classified according to WHO (26). Oligodendrogliomas and metastases were considered as individual tissue classes independently of grading or tissue of origin, respectively. Biopsies with ambiguous classifications were not included in the study. Specimen weight varied in the range 50–500 mg. Acid extracts were prepared from every biopsy (16, 19, 27), neutralized with KOH, lyophilized to dryness, and resuspended in D_2O (99.9% deuterium, approximately 100 mg of tissue/ml D_2O) just prior to ^{1}H MRS or amino acid analysis.

^{1}H MRS. ^{1}H MRS (360.13 MHz, pH 7.2, 22°C) was performed in a Bruker AM-360 spectrometer equipped with a commercial ^{1}H selective probe using 5-mm tubes and 0.5 ml of tissue extract. Acquisition conditions were: 90° pulses, 10 s total cycle time and 16,384 data points acquired in the time domain during an acquisition time of 1.90 s. The intensity of the residual water signal was reduced using a 2 s presaturating pulse centered on the water resonance. Prior to Fourier transformation, free induction decays were multiplied by an exponential function resulting in 0.1 Hz artificial line broadening in the transformed spectrum. Further spectral processing, including phase and baseline corrections was performed by the same operator. Chemical shifts were referred to the methyl signal of 2,2′-3,3′ tetradeutero trimethyl silyl propionate (TSP, 1 mM) at 0 ppm. Assignments were performed using literature values and were confirmed when necessary with the addition of the authentic compounds (7, 8, 16, 19, 27). Intensities of resonances were determined manually on spectra represented on an expanded scale and normalized for the amount of tissue extracted (Table 1, variables 1–27).

Amino Acid Analyses. Amino acid profiles of the biopsies were investigated in the same extracts used for ^{1}H MRS analysis by automatic ion exchange chromatography (Pharmacia, Upsalla, Sweden), using postcolumn derivatization with ninhydrin and spectrophotometric detection (28). A total of 17 amino acid concentrations were determined in every sample (Table 1, variables 28–44).

Statistical Analyses. Statistical analyses were performed using either the SAS system (SAS Institute Inc., Cary, NC) or the BMDP package (BMDP Statistical Software, Inc., Los Angeles, CA) as implemented on an ALPHA 2100 mainframe computer running under the VMS operating system (Digital Corp.). The experimental data set consisted of 81 extracts from biopsies distributed in the following histological classes: high-grade astrocytomas (n = 19, class 1); low-grade astrocytomas (n = 10, class 2); normal brain (n = 9, class 3); medulloblastomas (n = 4, class 4); meningiomas (n = 18, class 5); metastases (n = 8, class 6); neurinomas (n = 9, class 7); and oligodendrogliomas (n = 4, class 8). A total of 44 variables, consisting of 27 resonances or ratios of resonances measured by ^{1}H MRS and 17 amino acid concentrations measured by ionic exchange chromatography, were considered in the analyses.

First, a univariate analysis was performed in the complete data set consisting of 81 biopsies to determine basic statistics for every variable. Then, a step-wise discriminant analysis was carried out to search for the optimal combination of variables to discriminate between pairs of classes (29–31). Briefly, for a binary classification of a biopsy or group of biopsies between classes i and j, classification functions f_i and f_j (Eq. A and B) contain the linear combination of variables x_t that best discriminate between the classes compared.

$$f_i = \sum_{t=1}^{k} a_{it} x_t + a_0 \qquad \text{(A)}$$

$$f_j = \sum_{t=1}^{k} b_{jt} x_t + b_0 \qquad \text{(B)}$$

Classification functions contain independent terms as a_0 and b_0 and each variable is multiplied by a coefficient a_{it} or b_{jt} that reveals its statistical weight. No more than four variables were used in the classification ($k \leq 4$). The Fisher discriminant function F_{ij} describing this comparison is calculated as indicated in Eq. C, D, and E:

$$Z = \sum_{t=1}^{k} a_{it} x_t - \sum_{t=1}^{k} b_{jt} x_t \qquad \text{(C)}$$

$$C = a_0 - b_0 \qquad \text{(D)}$$

$$F_{ij} = Z + C \qquad \text{(E)}$$

Table 1 Basic statistics of the variables measured by ^{1}H MRS and amino acid analysis

Variable number	Variable name	ppm/retention time	n[a]	Mean ± SD (SE)
Intensities of resonances from specific protons of metabolites measured by ^{1}H MRS in biopsy extracts (Fig. 1).				
	^{1}H MRS variables[b]	ppm[c]		Resonance intensities[d]
1	NAAH6	2.01	79	1.76 ± 2.76 (0.31)
2	Cr,PCr (methyl)	3.05	79	5.11 ± 4.79 (0.54)
3	Cho (+PCho+GPCho)	3.20 (+3.23+3.24)	79	4.63 ± 3.20 (0.36)
4	Cr,PCr (methylene)	3.90	78	2.97 ± 2.60 (0.29)
5	InoH2	4.07	78	0.80 ± 1.11 (0.13)
6	LacH3	1.35	79	9.04 ± 5.04 (0.57)
7	AlaH3	1.55	79	1.56 ± 1.64 (0.18)
8	GluH3	2.05	79	1.73 ± 1.47 (0.17)
9	GlnH4	2.25	79	1.72 ± 1.59 (0.18)
10	TauH2	3.31	79	1.40 ± 1.73 (0.19)
11	GlyH2	3.60	79	2.77 ± 2.61 (0.29)
12	AcH2	1.90	79	2.00 ± 2.31 (0.26)
13	GluH4	2.35	79	3.23 ± 2.83 (0.32)
	Variables in ratios			Ratios of resonance intensities
14	Cho:Cr (methyl)		79	12.18 ± 63.80 (7.18)
15	Cho:InoH2		78	150.96 ± 250.87 (28.41)
16	Cho:NAAH6		79	143.43 ± 245.68 (27.64)
17	Cr,PCr (methyl):NAAH6		79	62.34 ± 123.22 (13.86)
18	GlnH4:GluH3		79	1.67 ± 5.56 (0.63)
19	TauH2:NAAH6		79	57.84 ± 102.59 (11.54)
20	InoH2:NAAH6		78	13.34 ± 52.98 (6.00)
21	AlaH3:NAAH6		79	85.12 ± 173.00 (19.46)
22	AlaH3:GlnH4			8.29 ± 34.55 (3.89)
23	GlyH2:NAAH6		79	70.16 ± 125.46 (14.12)
24	GlyH2:Cho		79	0.65 ± 0.37 (0.04)
25	GluH4:NAAH6		79	190.86 ± 200.27 (22.53)
26	GluH4:Cho		79	0.77 ± 0.51 (0.06)
27	GlyH2:InoH2		78	74.89 ± 112.88 (12.78)
Amino acid concentrations determined by automatic ionic exchange chromatography (Fig. 2).				
	Amino acid variables[e]	Retention time[f]		Concentrations[g]
28	*Asp*[e]	11.67	81	1981.00 ± 1669.30 (185.48)
29	*Gln*	14.33	81	4340.70 ± 3903.80 (433.75)
30	*Glu*	17.42	81	4072.70 ± 3848.30 (427.59)
31	*Gly*	23.83	81	1903.20 ± 2214.00 (246.00)
32	*Ala*	25.33	81	1530.10 ± 1850.10 (205.57)
33	*Cys*	26.92	81	318.32 ± 803.01 (89.22)
34	*Val*	27.83	81	1204.30 ± 2280.50 (253.38)
35	*Met*	29.83	81	151.67 ± 144.04 (16.00)
36	*Isoleu*	31.83	81	162.96 ± 121.99 (13.55)
37	*Leu*	33.17	81	279.80 ± 214.31 (23.81)
38	*Tyr*	37.42	81	193.38 ± 152.42 (16.94)
39	*Phe*	38.75	81	250.36 ± 211.52 (23.50)
40	*Hys*	45.00	81	219.43 ± 260.25 (28.92)
41	*Lys*	46.67	81	488.23 ± 552.4 (61.38)
42	*Arg*	58.00	81	192.88 ± 225.12 (25.01)
43	*Pro*	18.92	81	464.14 ± 447.19 (49.69)
44	*GABA*	40.33	81	232.37 ± 344.13 (38.24)

[a] *n*; the number of biopsies investigated for the corresponding variable.

[b] ^{1}H MRS variables: NAA, *N*-acetyl aspartic acid; Cr,PCr, creatine and phosphocreatine; Cho, choline; PCho, phosphorylcholine; GPCho, glycerolphosphorylcholine; Ino, inositol; Lac, lactate; Ala, alanine; Glu, glutamate; Gln, glutamine; Tau, taurine; Gly, glycine; Ac, acetate.

[c] The chemical shift of ^{1}H resonances is given in ppm with respect to the methyl resonance of 2,2′,3,3′ tetradeutero-trimethyl-sylil-propionate at 0 ppm.

[d] Resonance intensities are normalized for the amount of tissue extracted and are expressed in arbitrary units.

[e] Amino acid analysis variables (italic): *Asp*, aspartic acid; *Gln*, glutamine; *Glu*, glutamate; *Gly*, glycine; *Ala*, alanine; *Cys*, cisteine; *Val*, valine; *Met*, methionine; *Isoleu*, isoleucine; *Leu*, leucine; *Tyr*, tyrosine; *Phe*, phenylalanine; *Hys*, hystidine; *Lys*, lysine; *Arg*, arginine; *Pro*, proline; *GABA*, gamma aminobutyric acid.

[f] Minutes after the solvent injection front.

[g] Amino acid concentrations are given in nmol/g wet weight.

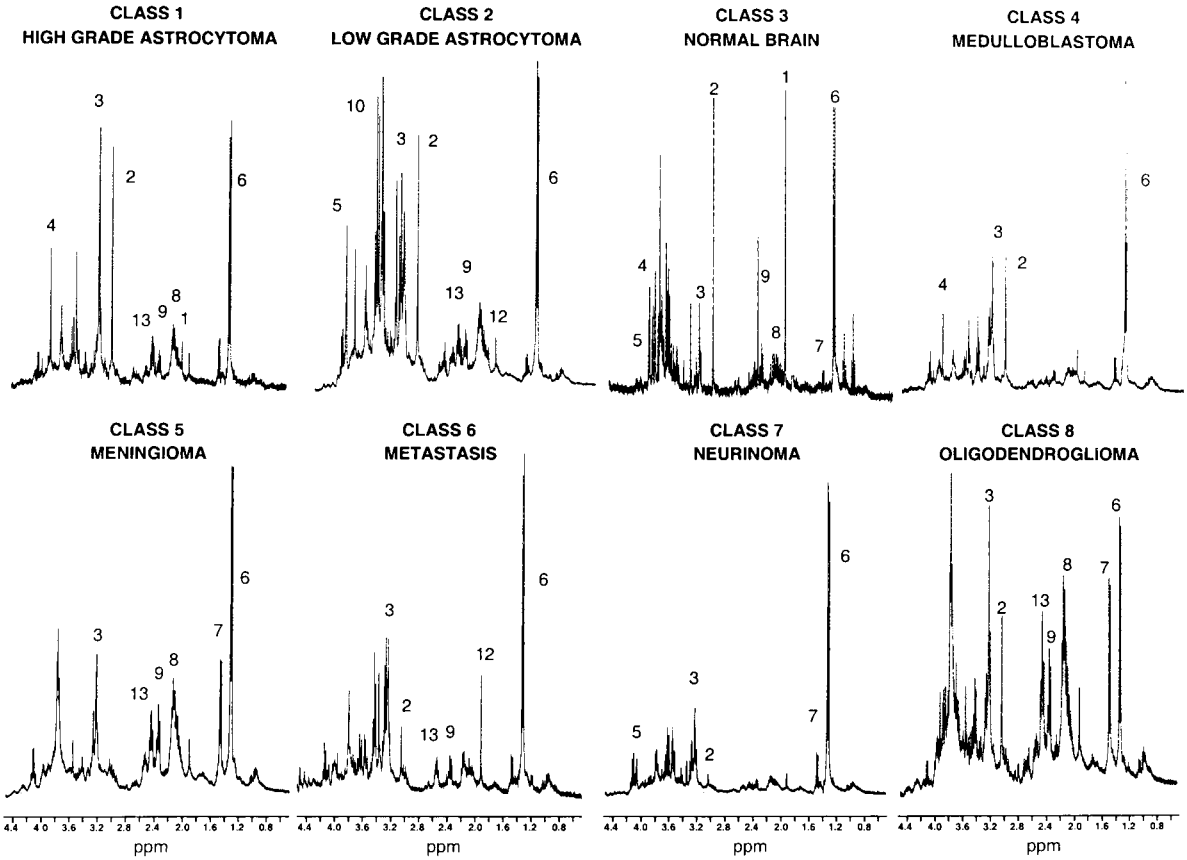

Fig. 1 ^{1}H MRS (369.13 MHz, 22°C, pH 7.2) of extracts from biopsies of the different tissue classes investigated in this study. *Numbers* in the spectra correspond to the variable numbers listed in Table 1.

For a binary comparison of a given extract of the database between tissue classes *i* and *j*, a positive value of the Fisher function F_{ij} classifies the extract in class *i*, and a negative value classifies the extract in class *j*. The probabilities that the investigated extract belongs to class *i* or *j* (p_i or p_j, respectively) are given by the expressions: $p_i = 1/[1+ \exp(-F_{ij})]$ or $p_j = 1 - p_i$, respectively.

The goodness of the Fisher discriminant function was tested using one of two methods: (*a*) by applying the function to all of the elements of the two classes compared and computing the number of correct classifications in each class; or (*b*) by using the LOO (or Jacknife) method. The latter protocol takes one of the elements of the two classes compared out of the data set, calculates the Fisher function with the remaining ones, and classifies the isolated element with the Fisher function calculated in its absence. The procedure is repeated with all of the elements of both classes, expressing the goodness of the Fisher functions as a score, or percentage of correct element classifications in each one of the two classes. The scores obtained for classes *i* and *j* do not necessarily need to be the same. This is the case because: (*a*) classes *i* and *j* may have different numbers of elements, resulting in different percentages of correct classifications, even if the same number of elements is classified correctly in both classes; or (*b*) classes *i* and *j* may have an identical number of elements, but correct classifications may be different in each class.

Binary classifications can be extended to multilateral comparison among *m* classes, where *m* in this case represents the eight classes considered in the present study. The final probability P_i that an extract from the database belongs to class *i* is given by the product of probability values calculated for all of the possible binary classifications of the extract between class *i* and the remaining ones (p_{im}). The following expression applies:

$$P_i = \prod^{m} p_{im},\ m = 1, 2, 3, \ldots 8 \qquad \text{(F)}$$

For every extract, this procedure yields one probability to belong to each one of the eight tissue classes considered, the extract being assigned to the class having the highest probability. In a well-defined classification, the probability to belong to one of the classes is much larger than the probability to belong to the others, and consequently, the degree of confidence in the assignment is high. If the calculated probability to belong to two classes of the multilateral comparison is similar, the conflict can be solved by using the corresponding binary comparison.

Materials. D_2O (99.9% deuterium) was purchased from Apollo Scientific (Stockport, England) and trimethyl silyl pro-

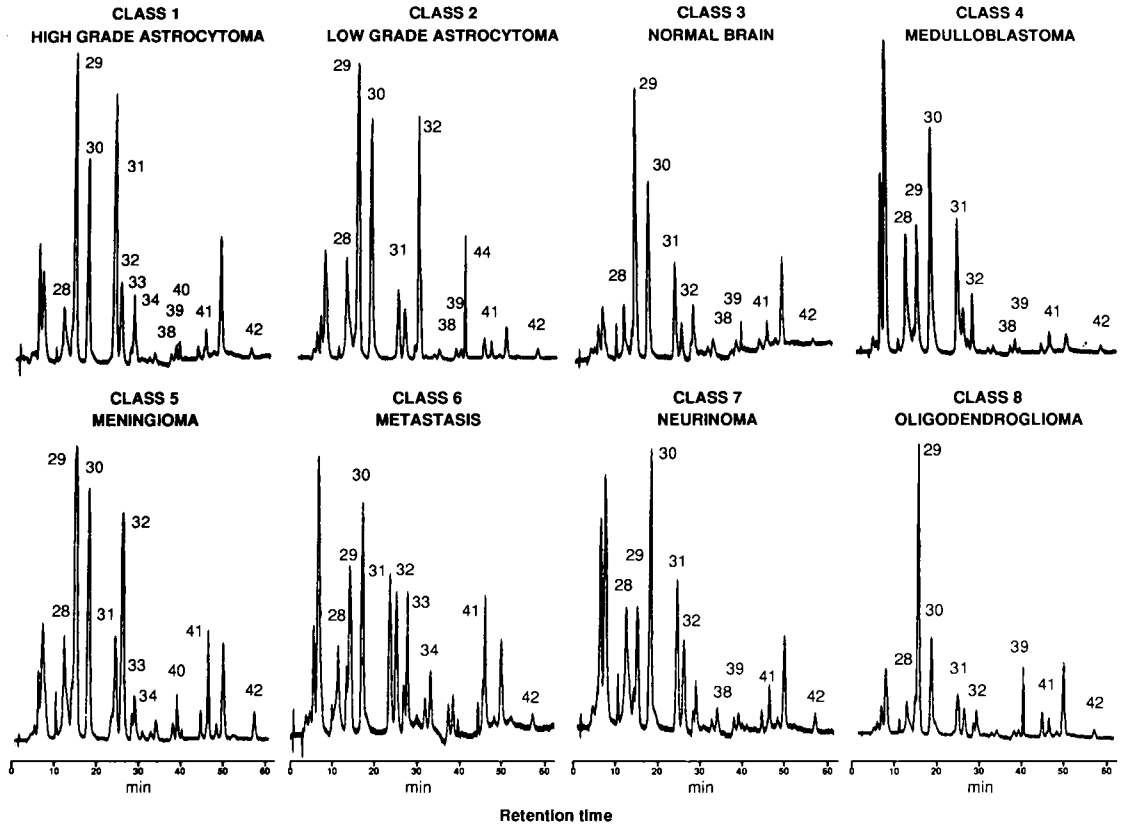

Fig. 2 Amino acid profiles obtained by automatic ionic exchange chromatography of extracts from biopsies of the different tissue classes investigated in this study. *Numbers* in the chromatograms correspond to the variable numbers listed in Table 1.

pionate was obtained from the company S.D.S. (Peypin, France). The rest of the reagents were of the highest quality available commercially.

RESULTS

^{1}H MRS and Amino Acid Analyses of Tumor Biopsies. Fig. 1 shows representative ^{1}H spectra from extracts of the different tissue classes examined in this study.

These spectra provide a fingerprint of the metabolite profiles of every tissue class. Detailed assignments of the resonances observed can be found in the literature (5, 13, 14, 19, 27). Briefly, a representative spectrum from normal brain/class 3 (27) shows as the most characteristic resonances: (*a*) those derived from the H6 hydrogens of *N*-acetyl aspartic acid (variable 1)[4]; (*b*) the methyl groups from creatine and phosphocreatine (variable 2); (*c*) the trimethyl ammonium groups of choline and derivatives (variable 3); (*d*) the methylene hydrogens from creatine and phosphocreatine (variable 4); (*e*) the H2 hydrogens of myoinositol (variable 5); (*f*) the H3 hydrogens of lactate (variable 6); and (*g*) the H3 hydrogens of alanine (variable 7). The remaining panels correspond to representative spectra from different classes of brain tumors, showing additional resonances (variables 8–13). ^{1}H MRS spectra of Fig. 1 reveal differences not only between normal brain and tumoral tissue but also among the different tumor classes. The normal brain is characterized by the high intensity of its *N*-acetyl aspartic H6 resonance (variable 1), which is lower in all tumor types and much lower or absent in the meningiomas. Meningiomas and oligodendrogliomas depict a higher alanine peak (variable 7) than the remaining tissue classes. Analysis of ratios between ^{1}H MRS resonances has also been proposed to provide a valuable tool for tumor classification (4, 7). Accordingly, we also evaluated the use of different ratios among intensities of resonances, as a criterion for tumor classification (Table 1, variables 14–27).

To complement ^{1}H MRS data, we performed amino acid analyses by ionic exchange chromatography in the same samples. Fig. 2 shows representative amino acid chromatograms from the various tissue classes under study. Notably, many amino acids that are difficult to detect or resolve by ^{1}H MRS appear clearly identified in the ion exchange chromatograms. This is the case for glutamine (variable 29) and glutamate (variable 30), glycine (variable 31), aspartate (variable 28), cysteine (variable 33), valine (variable 34), and tyrosine (variable 38), among others. As in Fig. 1, amino acid profiles revealed different metabolic patterns within the eight tissue classes considered. In particular, the glutamine (variable 29): glutamate(variable 30) ratio appears to be lower than one in

[4] Variable numbers refer to the variable numbers listed in Table 1 and shown in Fig. 1 and 2.

Table 2 Fisher functions (F) obtained for the binary classification of biopsy extracts from normal brain and different tumor types using ^{1}H MRS and amino acid analysis variables

Fisher discriminant functions for the binary comparison of classes i and j are given in the notation F_{ij}. Subscripts i and j indicate the two tissue classes compared: class 1, high grade astrocytomas; class 2, low grade astrocytomas; class 3, normal brain; class 4, medulloblastomas; class 5, meningiomas; class 6, metastasis; class 7, neurinomas; class 8, oligodendrogliomas. Abbreviations are those of Table 1.

$F_{12} = -1.6925$ InoH2 + 0.73475 AcH2 − 0.03124 *Tyr* + 0.00814 *Pro* + 3.80676
$F_{13} = 5.47087$ Cho/CrPCr (methyl) + 1.62179 AlaH3/GlnH4 − 4.37534
$F_{14} = 0.69163$ LacH3 − 9.65024 TauH2/NAAH6 + 4.80518
$F_{15} = 1.86284$ GlnH4 − 0.01807 Cho/NAAH6 − 0.18514 GlnH4/GluH3 − 0.01415 AlaH3/NAAH6 + 3.75059
$F_{16} = 1.30125$ Cho − 4.78298 TauH2 − 0.29660 AlaH3/GlnH4 + 3.6546
$F_{17} = 5.6539$ AlaH3 − 3.27157 TauH2 − 0.30072 InoH2/NAAH6 + 9.28088
$F_{18} = -2.7030$ TauH2/NAAH6 − 3.06133 InoH2/NAAH6 + 4.50546

$F_{23} = 0.00078$ *Gln* + 10.3793 Cho/CrPCr (methyl) + 1.11398 GlyH2/NAAH6 − 12.60783
$F_{24} = 1.6375$ GlnH4 − 4.24118 Cho/CrPCr (methyl) + 3.31323
$F_{25} = 1.57276$ Cho − 0.0227 Cho/NAAH6 − 3.50981
$F_{26} = 0.0168$ *Cis* − 0.1144 *Met* − 0.13481 Cho/InoH2 − 1.1418 AlaH3/NAAH6 + 39.067
$F_{27} = -0.0042$ *Gly* − 0.61331 CrPCr (methyl)/NAAH6 − 3.25047 AlaH3/GlnH4 + 38.6866
$F_{28} = -0.0050$ *Gly* − 1.75646 Cho/NAAH6 − 42.86 GluH4/Cho + 58.93676

$F_{34} = 2.27314$ GluH4 − 22.4706 Cho/CrPCr (methyl) + 15.88473
$F_{35} = 0.67874$ NAAH6 − 0.00847 Cho/NAAH6 − 0.08069
$F_{36} = -66.4354$ Cho/CrPCr (methyl) − 0.27227 Cho/InoH2 + 0.48885 TauH2/NAAH6 − 1.83245 AlaH3/NAAH6 + 98.294
$F_{37} = -14.954$ TauH2 − 1.54418 CrPCr (methyl)/NAAH6 − 9.12509 AlaH3/GlnH4 − 102.449
$F_{38} = -1.32412$ CrPCr (methyl)/NAAH6 + 5.46273

$F_{45} = -3.4786$ NAAH6 + 2.06735 Cho − 0.03057 Cho/NAAH6 − 1.84851
$F_{46} = 0.00620$ *Glu* + 0.10151 *GABA* − 15.7884
$F_{47} = -0.0125$ *Val* − 0.30997 CrPCr (methyl)/NAAH6 − 0.12323 InoH2/NAAH6 + 22.0757
$F_{48} = -17.2524$ CrPCr (methylene) − 0.00918 *Gln* + 106.699

$F_{56} = -0.01064$ *Tyr* + 0.00067 *Glu* + 0.00718 Cho/NAAH6 − 1.58002
$F_{57} = -1.1326$ TauH2 + 0.01851 *GABA* + 0.02226 Cho/CrPCr (methyl) + 0.04574 GlyH2/InoH2 − 4.26475
$F_{58} = -1.97727$ GluH4 + 0.01971 Cho/NAAH6 + 5.07561

$F_{67} = 2.3491$ Cho − 13.05543 InoH2 − 0.24284 InoH2/NAAH6 + 0.22508 AlaH3/NAAH6 − 1.2649
$F_{68} = -20.7371$ GluH4 + 0.04873 *Leu* + 59.7832

$F_{78} = 4.77238$ TauH2 − 13.6762 GluH4 + 44.3189

neurinomas and medulloblastomas but higher than one in the remaining tissue classes. Similarly, the glycine (variable 31): alanine(variable 32) ratio appears to be higher than one in most tissue classes and lower than one in low-grade astrocytomas and meningiomas. The following sections evaluate the statistical relevance of the changes observed in ^{1}H MRS and amino acid analysis variables within the eight tissue classes studied, as criteria for the classification of tumor biopsies *in vitro*.

Binary Classifications. Table 1 summarizes the mean, SD, and SE for every variable used in the comparisons, as computed using the complete data set containing all of the elements from the normal brain and the seven tumor classes. As expected, large variances are always obtained, indicating a large variation range of every variable among the different classes considered.

In a first approach, linear discriminant analysis was applied to determine the best combination of variables that would differentiate simultaneously among all of the tissue classes investigated using, at most, four variables. Using this strategy, it was possible to classify the complete data set into only two groups (100% success), normal brain and tumor pathologies; it was not possible to discriminate directly among the different tumor pathologies. In a second phase, binary comparisons were performed between every tissue class and each one of the remaining ones to select optimal variables for the classification, using: (*a*) only the MRS variables (variables 1–27, Table 1); (*b*) only the amino acid analysis variables (variables 28–44, Table 1); or (*c*) a combination of both (variables 1–44, Table 1). Every one of these comparisons considered all of the elements of both classes and resulted in a unique Fisher function as described in "Materials and Methods." Table 2 illustrates some of these results by showing the Fisher functions calculated using the combination of ^{1}H MRS and amino acid analysis variables.

Interestingly, the variables selected for every binary comparison were different, a circumstance explaining why it was not possible to classify the complete data set using a unique combination of the same four variables. Similarly, of the 17 amino acid concentrations investigated by ionic exchange chromatography, 11 were found to be involved in the binary classifications when considered together with MRS variables, which revealed that many amino acids contribute significantly to the discrimination process.

Table 3 provides the scores of binary comparisons obtained by the LOO method using only ^{1}H MRS variables, only amino acid analysis variables, or the combination of both (see Table 3, columns 2–9 and Table 2). Each row in Table 3 shows the results of binary comparisons between every tissue class and the remaining ones. The first row depicts the comparisons of high-grade astrocytomas (class 1). When compared with low-grade astrocytomas (class 2), Fisher functions—calculated using only ^{1}H MRS variables, or only amino acid variables, or both—classified correctly 15 (79%), 16 (84%), or 16 (84%) extracts of

Table 3 Scores obtained in the classifications of extracts between two possible tissue classes using ^{1}H MRS variables only, amino acid analysis variables only, or the combination of both

Table should be read following the rows. Every row lists the scores obtained in the binary classifications (LOO) of the elements of the tissue class indicated in the left column against the elements of each one of the other seven tissue classes. Each column shows the percentage of correct classifications obtained when the comparison is made using only variables measured by ^{1}H MRS (first of three percentages), only amino acid variables (second percentage) or a combination of both (third percentage). Classifications between two classes may yield different scores for each class, depending on the number of elements and the number of correct classifications in each class.

Tissue class	High-grade astrocytoma (class 1)	Low-grade astrocytoma (class 2)	Normal brain (class 3)	Medullo-blastoma (class 4)	Meningioma (class 5)	Metastasis (class 6)	Neurinoma (class 7)	Oligoden-droglioma (class 8)
High-grade astrocytoma (class 1, $n^a = 19$)		79, 84, 84	100, n.d., 100	100, 95, 100	100, 95, 100	100, 100, 100	95, 74, 100	89, 84, 89
Low-grade astrocytoma (class 2, $n = 10$)	70, 80, 90		90, 80, 90	90, 80, 90	90, 80, 90	100, 80, 100	90, 80, 100	90, 80, 100
Normal brain (class 3, $n = 9$)	100, 67, 89	89, 100, 100		100, 100, 100	100, 100, 100	100, 89, 100	100, 78, 100	100, 100, 100
Medulloblastoma (class 4, $n = 4$)	75, n.a., 75	75, 75, 75	100, 75, 100		50, 100, 50	75, 75, 100	100, n.a., 100	100, 100, 100
Meningioma (class 5, $n = 18$)	89, 72, 89	94, 89, 94	94, 61, 94	94, 61, 94		83, 94, 89	89, 72, 94	89, 67, 89
Metastasis (class 6, $n = 8$)	71, 75, 86	57, 87, 86	100, 75, 71	100, 100, 100	100, 87, 100		86, 62, 71	100, 100, 100
Neurinoma (class 7, $n = 9$)	100, 89, 100	86, 89, 86	100, 100, 100	86, n.a., 86	86, 89, 100	100, 100, 100		100, 100, 100
Oligodendroglioma (class 8, $n = 4$)	75, 75, 75	75, n.a., 100	75, 50, 75	100, 75, 100	100, n.a., 100	100, 100, 100	100, 100, 100	

[a] *n*, the number of elements in each class; n.d., not determined; n.a., not available.

the total of 19 extracts of class 1. The second row shows the comparisons of low-grade astrocytomas (class 2). In this case, when classified against high-grade astrocytomas, the same Fisher functions (used above) classified correctly 7 (70%), 8 (80%), or 9 (90%) extracts of the total of 10 extracts of class 2. Similar interpretations are applicable to the remaining rows and binary comparisons. In general, scores for the comparison of classes *i* and *j*, using F_{ij}, were not identical for both classes, as indicated in "Materials and Methods." ^{1}H MRS variables, when used exclusively, provided the best scores for correct classifications in 42 binary comparisons. Amino acid analysis variables, when used independently of ^{1}H MRS, gave highest scores in 18 binary comparisons. The combination of ^{1}H MRS and amino acid analysis variables yielded the highest scores in 52 of the 56 possible comparisons. Thus, the combination of ^{1}H MRS and amino acid analysis data provided a significant improvement over the scores reached by each method when used separately. In particular, important improvements were observed in the comparisons of low-grade with high-grade astrocytomas (from 70 to 90%; because of the contributions of tyrosine and proline) and in the comparisons between neurinomas and meningiomas (from 86 to 100%; attributable to *GABA*) or between oligodendrogliomas and low-grade astrocytomas (from 75 to 100%; attributable to glycine).

Graphs illustrating the binary comparison between high-grade astrocytomas and the remaining tissue classes are shown in Fig. 3. The figure shows as box plots, basic statistics of the variables selected for optimal discrimination chosen in each one of the comparisons. Similar plots were obtained for the remaining binary comparisons (not shown). Although considerable overlap exists among the means and SDs of the variables from the two classes being compared if the variables are considered individually, characteristic patterns or trends in the variables can be detected when considered as a group. Thus, high-grade astrocytomas present a different pattern of inositol and acetate resonances, tyrosine, and proline than do low-grade astrocytomas and present higher Cho:Cr ratios or AlaH3:GlnH4 ratios than does normal brain. These patterns are reflected in the corresponding Fisher functions calculated for each comparison (see Table 2).

Multilateral Classifications. The Fisher functions described in Table 2 also allow a multilateral classification of any arbitrarily chosen sample of the database against the eight possible tissue classes considered, as shown in Tables 4 and 5.

To accomplish this, the ^{1}H MRS and amino acid variables measured in the investigated sample (Table 4) are substituted in the appropriate Fisher functions (Table 2) providing numerical values for these functions in all of the possible binary comparisons and, thus, probabilities of assignment of the sample to each one of the two classes compared in every case (F_{ij}, p_{ij}, Table 5). The probability that the sample belongs to each one of the eight classes under investigation (P_1 to P_8) can be calculated as the product of probabilities of all binary comparisons involving the class considered (Eq. F). Briefly, the probability that an investigated biopsy belongs to class 1 (P_1) is the product of all probabilities $P_1 = p_{12} \cdot p_{13} \cdot p_{14} \cdot p_{15} \cdot p_{16} \cdot p_{17} \cdot p_{18}$, involving the possible binary comparisons of class 1 with the remaining seven classes. The probability to belong to classes P_2–P_8 can be calculated in a similar way. For the representative extract described in Tables 4 and 5, the calculated probabilities were: $P_1 = 0.860$; $P_2 = 8.147 \times 10^{-3}$; $P_3 = 9.873 \times 10^{-11}$; $P_4 = 1.91 \times 10^{-5}$; $P_5 = 1.173 \times 10^{-4}$; $P_6 = 5.546 \times 10^{-11}$; $P_7 = 1.663 \times 10^{-27}$; $P_8 = 6.277 \times 10^{-20}$, respectively. Thus, there is a much higher probability for this sample to belong to class 1 (high-grade astrocytomas). The remaining probabilities are much smaller, which indicates a large degree of confidence in

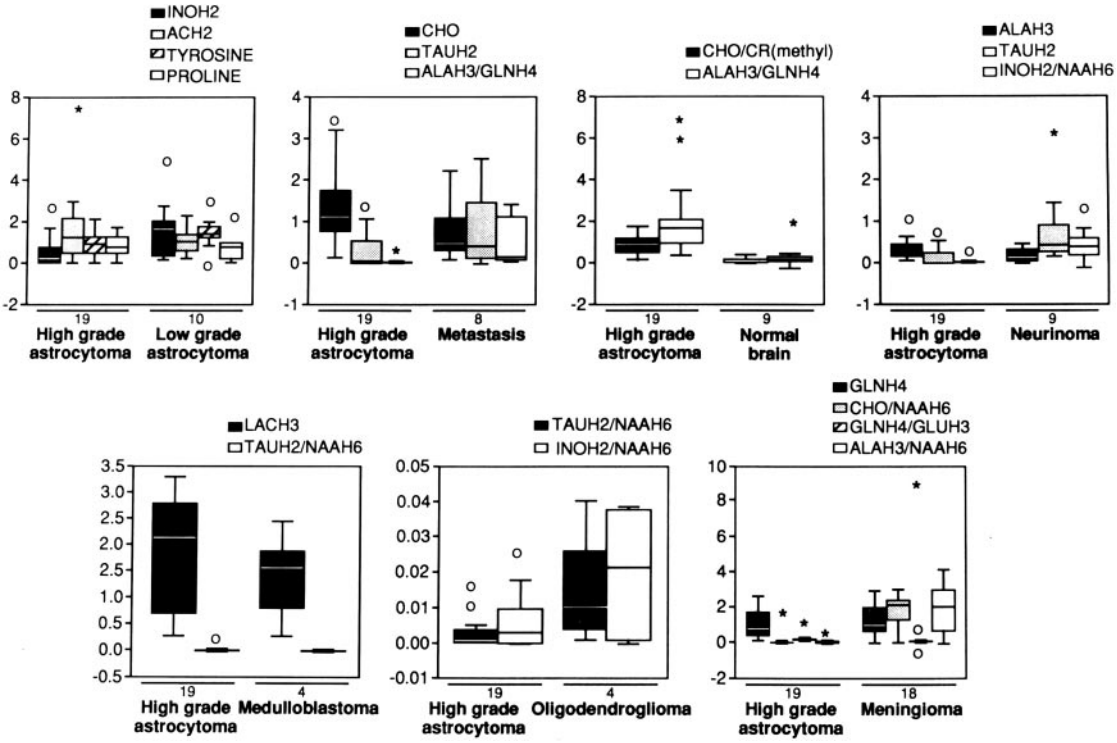

Fig. 3 Wiskers box-plots for the comparison of high-grade astrocytomas with the remaining seven tissue classes considered. A box of length equal to the interquartile range (IQR) contains 50% of the data between the upper and lower limits of the box. *Trace* (*horizontal line across each box*), the median of every class. *Upper and lower bars*, elements of the class located at a distance <1.5 times the IQR from the borders of the box. The remaining elements are considered outliers: ○, outliers within the expected outlier range; ∗, outliers outside the expected outlier range. Variable abbreviations are those of Table 1.

the classification as a class 1 biopsy. This same multilateral classification procedure was reproduced with the 81 biopsy extracts of the database, and the following scores of correct classifications were obtained: high-grade astrocytomas, 74%; low-grade astrocytomas, 80%; normal brain, 100%; medulloblastomas, 100%; meningiomas, 94.5%; metastases, 86%; neurinomas, 100%; and oligodendrogliomas, 75%.

DISCUSSION

We have presented a statistical multivariate approach for the nonhistological diagnosis of brain tumors *ex vivo*, combining ^{1}H MRS and amino acid profiles. An interesting aspect is that variables that we found to rank highest in the discrimination among the tissue classes were not ascribed sufficient relevance in previous reports. This has particular implications for the discrimination between high- and low-grade astrocytomas, a decision with important clinical consequences. Increased contents in choline (7), taurine (8), inositol (16), alanine, glycine, or phosphoethanolamine (7) were proposed earlier to be related to malignant degeneration of astrocytomas. Only some of these proposals could be confirmed in the present study. In particular, multivariate analysis of biopsy extracts did not find the choline resonances of extracts (considered as the combination of choline, phosphorylcholine, and glycerolphosphorylcholine resonances) of sufficient statistical weight to contribute to the discrimination between high- and low-grade astrocytomas. This finding represents an interesting difference from previous *in vivo* results, which traditionally attributed to the choline resonance a highly prognostic value (5, 14). A possibility accounting for the different *in vivo* and *in vitro* results is that the higher contribution of the choline resonance to some *in vivo* ^{1}H MRS classifications may be attributable to a population of highly mobile phospholipids, which is lost during the acid extraction process. In this respect, it is important to remark that *in vivo* ^{1}H MRS of some high-grade astrocytomas and glioblastomas often depicts a large peak of highly mobile neutral lipids, proposed earlier to be associated to intramembrane lipid microdomains or more recently to cytosolic lipid droplets (32–34). This mobile lipid resonance is lost during the extraction of acid soluble metabolites and, therefore, is not considered by *in vitro* classifications.

Our results indicate that inositol and acetate resonances contribute dominantly to the discrimination between biopsy extracts of high-grade and low-grade astrocytomas. These findings agree with previous work reporting inositol as the most important variable in this discrimination (19). Acetate is also a significant contributor to this discrimination, probably because the low oxidative capacity of astrocytic tumors, which could result in an accumulation of this precursor of the tricarboxylic acid cycle. Intense acetate signals, together with increased branched-chain amino acid concentrations, have also been reported previously to be associated to bacterial infections (35).

Table 4 Values of ^{1}H MRS and amino acid analysis variables needed for a representative multilateral classification

Variable numbers and abbreviated names are those of Table 1.

Variable number	Variable name	Value
	^{1}H MRS variables	Resonance intensities[a]
1	NAAH6	0.900
2	CrPCr (methyl)	2.100
3	Cho	2.200
4	CrPCr (methylene)	1.300
5	InoH2	0.000
6	LacH3	4.600
7	AlaH3	0.700
8	GluH3	0.800
9	GlnH4	1.100
10	TauH2	0.000
11	GlyH2	3.300
12	AcH2	1.400
13	GluH4	1.800
	Variables in ratios	Ratios of resonance intensities[a]
14	Cho:CrPCr (methyl)	1.050
15	Cho:InoH2	220.0
16	Cho:NAAH6	2.444
17	CrPCr (methyl):NAAH6	2.333
18	GlnH4:GluH3	1.3750
19	TauH2:NAAH6	0.000
20	InoH2:NAAH6	0.000
21	AlaH3:NAAH6	0.7778
22	AlaH3:GlnH4	0.6364
23	GlyH2:NAAH6	3.6667
24	GlyH2:Cho	1.500
25	GluH4:NAAH6	2.000
26	GluH4:Cho	0.8182
27	GlyH2:InoH2	330.0
	Amino acid variables	Amino acid concentrations[b]
29	*Gln + Ser*	3255.2856
31	*Gly*	3825.3579
33	*Cys*	174.9328
34	*Val*	246.7949
35	*Met*	52.7966
37	*Leu*	127.0453
38	*Tyr*	190.4100
43	*Pro*	517.5107
44	*GABA*	167.0433

[a] Resonance intensities or ratios of resonance intensities (variables 1–27) are given in arbitrary units.

[b] Amino acid concentrations (variables 29–44) are expressed in nmol/g wet weight.

Table 5 Values of the Fisher functions (F) and associated probabilities calculated for all possible binary comparisons of the biopsy from Table 4 with the eight brain tissue classes studied

Tissue classes compared i/j[a]	F_{ij}[b]	p_i[c]
1/2	3.100	0.957
1/3	2.388	0.916
1/4	7.987	1.000
1/5	5.490	0.996
1/6	6.329	0.998
1/7	13.239	0.999
1/8	4.505	0.989
2/3	4.889	0.993
2/4	0.671	0.662
2/5	−0.105	0.474
2/6	5.420	0.996
2/7	19.121	0.999
2/8	0.449	0.610
3/4	−3.564	0.028
3/5	0.509	0.625
3/6	−32.630	0.000
3/7	93.039	0.999
3/8	2.373	0.915
4/5	−0.506	0.376
4/6	25.656	0.999
4/7	18.268	0.999
4/8	54.387	0.999
5/6	−0.942	0.280
5/7	13.945	0.999
5/8	1.565	0.827
6/7	4.078	0.983
6/8	28.647	0.999
7/8	19.702	0.999

[a] Tissue class numbers are those of Fig. 1 and 2.

[b] Numerical values for the Fisher functions F_{ij} used in the comparison of classes i and j are calculated using the Fisher functions of Table 2 and the variables from Table 4.

[c] In the comparison of classes i and j, the probability of the sample to belong to class i is $p_i = 1/(1 + \exp(-F_{ij}))$ and the probability to belong to class j is $p_j = 1 - p_i$. Only the values of p_i for comparisons where $j > i$ are shown. The remaining can be calculated as $1 - p_i$.

Nevertheless, a crucial aspect highlighted by the present study is that optimal discrimination between astrocytic tumor grades cannot be based exclusively on the inositol or acetate resonances, or on any of the four variables involved in the discriminant function, when considered individually. It demands the linear combination of all of these variables weighted by the appropriate factors, a circumstance reflecting the complexity in the decision process and applicable also to the remaining comparisons.

Notably, the amino acids tyrosine and proline become relevant contributors to the discrimination between high- and low-grade gliomas. Some other amino acids such as glutamine, cysteine, glycine, glutamate, valine, and taurine provide similar improvements with other classifications. Of these amino acids, glutamine is the most important variable in the discrimination between: high-grade astrocytomas and meningiomas, low-grade astrocytomas and normal brain, and low-grade astrocytomas and medulloblastomas. This may be attributable in part to the increased metabolism of glutamine reported in tumors (36), as compared with normal brain (8), a proposal that matches well with the high rates of glutamine consumption and glutamate release reported for experimental gliomas (37, 38). Taken together, these observations reveal that the alterations in glutamine and glutamate homeostasis observed in tumors (22–24) may have clear diagnostic implications. Glycine is shown to contribute dominantly to the discrimination between low-grade astrocytomas and neurinomas and between low-grade astrocytomas and oligodendrogliomas. Earlier ^{1}H MRS studies showed increased glycine concentrations in gliomas and medulloblastomas (6) or glioblastomas (7, 12). Augmented glycine content may be derived in these cases from increased phosphatidylcho-

line turnover and decreased oxidative capacity. The high taurine content of neurinomas makes this amino acid the dominant contributor to the identification of this type of tumor and its discrimination from metastases and medulloblastomas. Finally, valine, methionine, cysteine, tyrosine, and proline, a series of amino acids that have not been evaluated previously in the ^{1}H MRS analysis of tumor biopsies, are shown here to contribute importantly to some discriminations. Interestingly, increased tumoral uptake of tyrosine and methionine derivatives labeled with ^{18}F or ^{11}C, respectively, have been proposed as diagnostic tests for tumor imaging by positron emission tomography (39, 40). In summary, present results reveal characteristic differences in amino acid metabolism among different tumor types, which may be exploited for diagnostic purposes.

Finally, a relevant aspect is the comparison of the scores obtained with the present study with scores provided by alternative procedures (3, 21, 41–44). Using neural networks (19), it was previously possible to obtain correct glioma discrimination within two grades in 79% of the tests, whereas the present approach yields 84–90% correct classifications in the same comparison. The percentage of correct classifications with the present method was also higher in almost all of the other comparisons, reaching 100% in many cases. Similar results were reported by Somorgay *et al.* (89–100%; Ref. 20) and Martínez-Pérez *et al.* (80%; Ref.44) using linear discriminant analysis or pattern recognition techniques, respectively. However, a relevant advantage of the proposed multivariate analysis method is that it allows investigators, for the first time to our knowledge, to classify any sample of the database within the eight different tissue classes considered, previous multivariate approaches providing mainly binary classifications. Notably, the percentages of correct scores in multilateral comparisons are not much smaller than those found in binary comparisons. In this respect, it should be emphasized here that multilateral comparisons present more stringent requirements for a correct classification than binary comparisons, when considering the effects of chance. A classification by chance of a biopsy between two classes would provide 50% correct scores, but classification of the same biopsy among the eight classes considered would provide only 12.5% correct scores. Thus, although the scores of multilateral comparisons are in some cases lower than in bilateral comparisons, they represent a higher accuracy in the classification process, when considering the effects of chance.

In summary, the results presented here provide a promising background for the implementation of nonhistological protocols for *ex vivo* tumor diagnosis in clinical settings. Further progress toward this end demands several improvements to be made, including an increase in the number of samples of the database, exploration of additional biochemical or genetic variables for discriminant analysis, and an automation procedure directly linking analytical acquisitions and processing with biopsy classification. Histological procedures remain mandatory for tumor diagnosis. However, pathologists may find these alternative protocols useful in cases where a confirmation of the histological diagnosis by an independent method is advisable or in situations in which adequate anatomopathological examinations cannot be performed.

ACKNOWLEDGMENTS

We thank the members of the Neurosurgical Service from the University Hospital La Paz for their contributions to the obtaining of tissue samples from the operating theater and to Dr. Cristina Santa Marta for helpful comments and critical reading of the manuscript.

REFERENCES

1. Bigner, S. H., McLendon, R. E., Al-dosari, N., and Rasheed, A. Brain tumors. *In:* B. Vogelstein and K. W. Kinzler (eds.), The Genetic Basis of Human Cancer, pp. 661–670. New York: McGraw-Hill, Inc., 1998.

2. Spence, A. M. Lactic dehydrogenase in ethylnitrosourea rat gliomas. Total lactic dehydrogenase activity and isozymes in autochthonous gliomas and cloned transplantable astrocytomas. Oncology (Basel), *36:* 260–264, 1979.

3. Hagberg, G., Burlina, A., Mader, I., Roser, W., Radue, E. W., and Seelig, J. *In vivo* proton MR spectroscopy of human gliomas: definition of metabolic coordinates for multidimensional classification. Magn. Reson. Med., *34:* 242–252, 1995.

4. Preul, M. C., Caramanos, Z., Collins, D. L., Villemure, J-G., Leblanc, R., Olivier, A., Pokrupa, R., and Arnold, D. L. Accurate, noninvasive diagnosis of human brain tumors by using proton magnetic resonance spectroscopy. Nat. Med., *2:* 323–325, 1996.

5. Tedeschi, G., Lundbom, N., Raman, R., Bonavita, S., Duyn, J. H., Alger, J. R., and Di Chiro, G. Increased choline signal coinciding with malignant degeneration of cerebral gliomas: a serial proton magnetic resonance spectroscopy-imaging study. J. Neurosurg., *87:* 516–524, 1997.

6. Kinoshita, Y., Kajiwara, H., Yokota, A., and Koga, Y. Proton magnetic resonance spectroscopy of brain tumors: an *in vitro* study. Neurosurgery (Baltimore), *35:* 606–614, 1994.

7. Kinoshita, Y., and Yokota, A. Absolute concentrations of metabolites in human brain tumors using *in vitro* proton magnetic resonance spectroscopy. NMR Biomed., *10:* 2–12, 1997.

8. Peeling, J., and Sutherland, G. High resolution ^{1}H NMR spectroscopy studies of extracts from cerebral neoplasms. Magn. Reson. Med., *24:* 123–136, 1992.

9. Hagberg, G. From magnetic resonance spectroscopy to classification of tumors. A review of pattern recognition methods. NMR Biomed., *11:* 148–156, 1998.

10. Negendank, W. Studies of human tumors by MRS. A review. NMR Biomed., *5:* 303–324, 1992.

11. Sutton, L. N., Wehrli, S., Gennarelli, L., Huang, Z., Zimmerman, R., Bonner, K., and Rorke, L. B. High resolution ^{1}H magnetic resonance spectroscopy of pediatric posterior fossa tumors *in vitro*. J. Neurosurg., *81:* 443–448, 1994.

12. Carpinelli, G., Carapella, C. M., Palombi, L., Raus, L., Caroli, F., and Podo, F. Differentiation of glioblastoma multiforme from astrocytomas by *in vitro* ^{1}H MRS analysis of human brain tumors. Anticancer Res., *16:* 1559–1564, 1996.

13. Gill, S. S., Thomas, D. G. T., Van Bruggen, N., Gadian, D. G., Peden, C. J., Bell, J. M., Cox, I. J., Menon, D. K., Iles, R. A., Briant, D. J., and Coutts, G. A. Proton MR Spectroscopy of intracranial tumours: *in vivo* and *in vitro* studies. J. Comput. Assisted Tomogr., *14:* 497–504, 1990.

14. Usenius, J. P., Vainio, P., Hernesniemi, J., and Kauppinen, R. Choline containing compounds in human astrocytomas studied by ^{1}H NMR spectroscopy *in vivo* and *in vitro*. J. Neurochem., *63:* 1538–1543, 1994.

15. Usenius, J. P., Kauppinen, R. A., Vainio, P. A., Hernesniemi, J. A., Vapalahti, M. P., Paljarvi, L. A., and Soimakallio, S. Quantitative metabolite patterns of human brain tumors: detection by ^{1}H NMR spectroscopy *in vivo* and *in vitro*. J. Comput. Assisted Tomogr., *18:* 705–713, 1994.

16. Pascual, J. M., Carceller, F., Cerdán, S., and Roda, J. M. Diagnóstico diferencial de tumores cerebrales "*in vitro*" por espectroscopía de resonancia magnética de protón. Método de los cocientes espectrales. Neurocirugía (Santiago), *9:* 4–10, 1998.

17. Tate, A. R., Griffiths, J. R., Martínez-Pérez, I., Moreno, A., Barba, I., Cabañas, M., Watson, D., Alonso, J., Bartumeus, F., Isamat, F., Ferrer, I., Vila, F., Ferrer, E., Capdevilla, A., and Arús, C. Towards a method for automated classification of 1H MRS spectra from brain tumors. NMR Biomed., *11:* 177–191, 1998.

18. Lisboa, P. J. B., Kirby, S. P. J., Vellido, A., Lee, Y. Y. B., and El-Deredy, W. Assessment of statistical and neural networks methods in NMR spectral classification and metabolite selection. NMR Biomed., *11:* 225–234, 1998.

19. Maxwell, R. J., Martinez-Pérez, I., Cerdán, S., Cabañas, M. E., Arús, C., Moreno, A., Capdevilla, A., Ferrer, E., Bartomeus, F., Aparicio, A., Conesa, G., Roda, J. M., Carceller, F., Pascual, J. M., Howells, S., Mazucco, R., and Griffiths, J. R. Pattern recognition analysis of ^{1}H NMR spectra from perchloric acid extracts of human brain tumour biopsies. Magn. Reson. Med., *39:* 869–877, 1998.

20. Somorjai, R. L., Dolenko, B., Nikulin, A. K., Pizzi, N., Scarth, G., Zhilkin, P., Halliday, W., Fewer, D., Hill, N., Ross, I., West, M., Smith, I. C. P., Donnelly, S. M., Kuesel, A. C., and Brière, K. M. Classification of ^{1}H MR spectra of human brain neoplasms: the influence of preprocessing and computerized consensus diagnosis on classification accuracy. J. Magn. Reson. Imaging, *6:* 437–444, 1996.

21. Tate, A. R. Statistical pattern recognition for the analysis of biomedical magnetic resonance spectra. J. Magn. Reson. Anal., *3:* 63–78, 1997.

22. Marquez, J., Sanchez-Jimenez, F., Medina, M. A., Quesada, A. R., and Nuñez de Castro, I. Nitrogen metabolism in tumor bearing mice. Arch. Biochem. Biophys., *268:* 667–675, 1989.

23. Pisters, P. W., and Pearlstone, D. B. Protein and amino acid metabolism in cancer cachexia: investigative techniques and therapeutic interventions. Crit. Rev. Clin. Lab. Sci., *30:* 223–272, 1993.

24. Rivera, S., Azcon-Bieto, J., López-Soriano, F. J., Miralpeix, M., and Argiles, J. M. Amino acid metabolism in tumor bearing mice. Biochem. J., *249:* 443–449, 1988.

25. Daumas-Duport, C., Scheithauer, B. W., O'Fallon, J., and Kelly, P. Grading of astrocytomas: a simple and reproducible methods. Cancer (Phila.), *62:* 2152–2165, 1988.

26. Kleihues, P., Burger, P. C., and Scheithauer, B. W. Histologic Typing of Tumors of the Central Nervous System. Berlin: Springer-Verlag, 1993.

27. Cerdán, S., Parrilla, R., Santoro, J., and Rico, M. ^{1}H NMR detection of cerebral myoinositol. FEBS Lett., *187:* 167–172, 1985.

28. Speckman, D. H., Stein, W. H., and Moore, S. Automatic recording apparatus for the use in the chromatography of amino acids. Anal. Chem., *30:* 1190–1206, 1958.

29. Afifi, A. A., and Clark, V. Computer-aided Multivariate Analysis. Belmont, CA: Lifetime Learning Publications, 1990.

30. Fisher, R. A. The use of multiple measurements on taxonomic problems. Ann. Eugenics, *7:* 179–188, 1936.

31. Tabachnick, B. G., and Fidell, L. S. Using Multivariate Statistics. New York: Harper and Row, 1983.

32. Mountford, C. E., and Wright, L. C. Organization of lipids in the plasma membranes of malignant and stimulated cells: a new model. Trends Biochem. Sci., *13:* 172–177, 1988.

33. Remy, C., Fouilhé, N., Barba, I., Sam-Laï, E., Lahrech, H., Cucurella, M- G., Izquierdo, M., Moreno, A., Ziegler, A., Massarelli, R., Décorps, M., and Arús, C. Evidence that mobile lipids detected in rat brain glioma by ^{1}H nuclear magnetic resonance correspond to lipid droplets. Cancer Res., *57:* 407–414, 1997.

34. Barba, I., Cabañas, M. E., and Arús, C. The relationship between nuclear magnetic resonance-visible lipids, lipid droplets, and cell proliferation in cultured C6 cells. Cancer Res., *59:* 1861–1868, 1999.

35. Martínez-Pérez, I., Moreno, A., Alonso, J., Aguas, J., Conesa, G., Capdevilla, A., and Arús, C. Diagnosis of brain abscess by magnetic resonance spectroscopy. J. Neurosurg., *86:* 708–713, 1997.

36. Medina, M. A., Sanchez-Jimenez, F., Márquez, J., Rodriguez-Quesada, A., and Nuñez de Castro, I. Relevance of glutamine metabolism to tumor cell growth. Mol. Cell. Biochem., *113:* 1–15, 1992.

37. Bowzier, A. K, Quesson, B., Valeins, H., Canioni, P., and Merle, M. (1-^{13}C) glucose metabolism in the tumoral and nontumoral cerebral tissue of a glioma bearing rat. J. Neurochem., *72:* 2445–2455, 1999.

38. Ye, Z-C., and Sontheimer, H. Glioma cells release excitotoxic concentrations of glutamate. Cancer Res., *59:* 4383–4391, 1999.

39. Inoue, T., Shibashaki, T., Oriuchi, N., Aoyagi, K., Tomiyoshi, K., Amano, S., Mikuni, M., Ida, I., Aoki, J., and Endo, K. ^{18}F α-methyl tyrosine PET studies in patients with brain tumors. J. Nucl. Med., *40:* 399–405, 1999.

40. Namba, H., Iwadate, Y., Iyo, M., Fukushi, K., Irie, T., Sueyosi, K., Tagawa, M., and Sakiyama, S. Glucose and methionine uptake by rat brain tumor treated with prodrug-activated gene therapy. Nucl. Med. Biol., *25:* 247–250, 1998.

41. Howells, S. L., Maxwell, R. J., Peet, A. C., and Griffiths, J. R. An investigation of tumor ^{1}H nuclear magnetic resonance spectra by the application of chemometric techniques. Magn. Reson. Med., *28:* 214–236, 1992.

42. Howells, S. L., Maxwell, R., and Griffiths, J. R. An investigation of tumor ^{1}H NMR spectra by pattern recognition. NMR Biomed., *5:* 59–64, 1992.

43. Kari, S., Olsen, N. J., and Park, J. H. Evaluation of muscle diseases using artificial neural network analysis of ^{31}P MR spectroscopy data. Magn. Reson. Med., *34:* 664–672, 1995.

44. Martínez-Pérez, I., Maxwell, R. J., Howells, S. L., van den Bogaart, A., Mazucco, R., Griffiths, J. R., and Arús, C. Pattern recognition analysis of ^{1}H NMR spectra from human brain tumour biopsies. Proc. Soc. Magn. Reson., 3rd Annual Meeting. Abstract P1709, 1995.